



EUROPEAN ORGANIZATION FOR NUCLEAR RESEARCH

CERN-EP/83-48  
March 23rd, 1983

EXPERIMENTAL DETERMINATION OF THE  $\pi$  MESON STRUCTURE  
FUNCTIONS BY THE DRELL-YAN MECHANISM.

NA3 COLLABORATION

J. Badier<sup>4</sup>, J. Boucrot<sup>5</sup>, J. Bourotte<sup>4</sup>, G. Burgun<sup>1</sup>, O. Callot<sup>5</sup>,  
Ph. Charpentier<sup>1</sup>, M. Crozon<sup>3</sup>, D. Decamp<sup>5</sup>, P. Delpierre<sup>3</sup>, B. Gandois<sup>1</sup>,  
R. Hagelberg<sup>2</sup>, M. Hansroul<sup>2</sup>, Y. Karyotakis<sup>5</sup>, W. Kienzle<sup>2</sup>, P. Le Dû<sup>1</sup>,  
J. Lefrançois<sup>5</sup>, Th. Leray<sup>3</sup>, J. Maillard<sup>3</sup>, G. Matthiae<sup>2</sup>, A. Michelini<sup>2</sup>,  
Ph. Miné<sup>4</sup>, G. Rahal<sup>1</sup>, O. Runolfsson<sup>2</sup>, P. Siegrist<sup>1</sup>, A. Tilquin<sup>3</sup>,  
J. Timmermans<sup>2</sup>, J. Valentin<sup>3</sup>, R. Vanderhaghen<sup>4</sup>, S. Weisz<sup>4</sup>.

CEN, Saclay<sup>1</sup>-CERN, Geneva<sup>2</sup>-Collège de France, Paris<sup>3</sup>-  
Ecole Polytechnique, Palaiseau<sup>4</sup>-Laboratoire de l'Accélérateur Linéaire, Orsay<sup>5</sup>.

ABSTRACT

We have studied high statistics samples of dimuon events ( $\sim 35\,000$ ) produced from  $\pi^\pm$  on platinum target in the mass interval  $4.2 \leq M_{\mu\mu} \leq 8.5$  GeV at 150, 200 and 280 GeV/c. The  $\pi$  structure function is obtained by a fit of  $d^2\sigma/dx_1 dx_2$  to  $\pi^+$  and  $\pi^-$  data. At 200 GeV, the simultaneous use of  $\pi^+$  and  $\pi^-$  data allows a separate determination of the valence and sea structure functions of the  $\pi$ . Furthermore, the 150 and 280 GeV data allow an accurate determination of the shape of the valence structure function and give an estimate of its evolution between  $Q^2 = 25$  and  $50$  GeV<sup>2</sup>.

---

Submitted to Zeitschrift für Physik C

This paper presents the final analysis of the pion structure investigated by measuring  $\mu$  pair production by  $\pi^{\pm}$  at 200 GeV/c and  $\pi^{-}$  at 150 and 280 GeV/c on a platinum target. An important feature of the Drell-Yan mechanism [1] in the quark parton model is the possibility to extract quark structure functions and specially those of unstable particles, as  $\pi$  and  $K$ , which cannot be studied by deep inelastic scattering (DIS) of leptons. In the framework of QCD, when the gluon corrections responsible for scaling violation are computed [2], it is found that, in the leading log approximation, the usual Drell-Yan cross section formula still remains valid, except for the replacement of the scaling structure functions by  $Q^2$  dependent structure functions according to the Altarelli-Parisi equations. These functions are the same in Drell-Yan and DIS processes. However, deviations from the standard Drell-Yan formula arise when one computes the first order QCD corrections, including next to leading log terms [3]. In this framework the predicted dimuon production cross section is found larger than the usual Drell-Yan prediction by a factor  $K$  which is nearly independent of the rapidity and of the mass in the limited range covered by experiments. Computations at the second order or attempts of exponentiation give the same prediction with a higher value of the  $K$  factor. In summary, at least at the 1<sup>st</sup> order of QCD corrections, the factorization property is preserved, (the cross section being just proportional to the parton-model Drell-Yan cross section). Recently, several theoretical groups studied the problem of initial state interactions [4] and some of them pointed out that this effect could destroy the factorization in the Drell-Yan formula or give different structure functions in Drell-Yan and DIS processes, but this is still controversial.

Experimentally, it is then crucial to test the factorization and to compare the nucleon structure function obtained in Drell-Yan and in DIS experiments. In previous papers [5], we have given the results of measurements of the Drell-Yan absolute cross section and of the shape of the nucleon structure functions by the analysis of massive dimuons events produced by antiprotons at 150 GeV and by protons at 150 and 200 GeV/c. Good agreement was found with the results obtained in DIS experiments for the shape of the valence structure function, the measured cross sections exceeding the predictions of the simple Drell-Yan model by an overall

normalization factor  $K = 2.3 \pm 0.4$ . We are then confident that we can use the Drell-Yan formula, assuming factorization and constant K factor, to extract the shape of the  $\pi$  structure functions from our  $\pi$  data.

## 1) EXPERIMENTAL DATA

Our experimental set up at the CERN SPS has been described previously [6]. The muon pairs are produced in a 6 cm platinum target placed 40 cm upstream of the 1.5 m hadron absorber. The muons are analysed by our multiwire proportional chamber magnet spectrometer. The  $K^-$  and  $\bar{p}$  in the negative beam are identified by differential Cerenkov counters (Cedar). For the positive beam, the  $\pi^+$ , p,  $K^+$  separation is performed by Cedar and threshold Cerenkov counters. The relative  $\pi^+/\pi^-$  luminosity is monitored by the  $J/\psi$  events collected simultaneously with the dimuon continuum. The  $J/\psi$  production cross section by  $\pi^+$  and  $\pi^-$  beams on a platinum target were measured to be equal within  $\pm 1\%$ . The  $\pi^+/\pi^-$  relative luminosity is thus known to  $\pm 2\%$ .

## 2) SELECTION OF EVENTS

The resolution on the dimuon mass being about 4%, we select events with mass in the range 4.2 to 8.5  $\text{GeV}/c^2$  to exclude the resonances region ( $J/\psi$ ,  $\psi'$ ,  $T$ ). In order to eliminate events produced by secondary interactions in the platinum target and since this background is small at  $x_F > 0$  but rapidly increasing at negative  $x_F$ , we perform a second selection  $x_F > -0.1$ . Another source of background is due to  $J/\psi$  events produced in the hydrogen target and wrongly reconstructed in the platinum target with a mass larger than 4  $\text{GeV}/c^2$ . This contamination comes essentially from asymmetrical dimuons which can be eliminated by a cut on  $\cos\theta^*$ :  $|\cos\theta^*| < 0.5$ . This selection eliminates a small fraction of events since the acceptance for  $|\cos\theta^*| > 0.5$  is rather small.

Finally, we eliminate the  $(x_1, x_2)$  regions where the acceptance is smaller than 3%. Having applied all these cuts, the number of dimuon events at different energies and for different incident particles are given in table 1.

### 3) METHOD OF ANALYSIS

#### 3.1 The quark annihilation model

The muon pair momentum  $p^*$  and the invariant mass  $M_{\mu\mu}$  determine the kinematical variables of the annihilating  $\bar{q}q$  pair :

$$M_{\mu\mu}^2 = x_1 x_2 s \quad X = x_1 - x_2 = \frac{2P^*}{\sqrt{s}}$$

where  $x_1$  and  $x_2$  are the fractional momenta of the quark in the beam and target particle respectively, neglecting the transverse momenta of the quarks. This approximation introduces an error on  $x_1$  and  $x_2$  of the order of 1%, which is much smaller than experimental errors. In the Drell-Yan model, the differential cross-section is given by :

$$\frac{d^2\sigma}{dx_1 dx_2} = \frac{\sigma_0}{3x_1 x_2} \sum_i \frac{Q_i^2}{x_1 x_2} [f_i^{h^1}(x_1) f_{\bar{i}}^{h^2}(x_2) + f_{\bar{i}}^{h^1}(x_1) f_i^{h^2}(x_2)] \quad (1)$$

where the sum is over different quark flavours;  $f_i^h(x)$ ,  $f_{\bar{i}}^h(x)$  are the quark and antiquark structure functions of flavor  $i$  in the hadron  $h$ ;  $Q_i$  is the quark charge, and  $\sigma_0 = (4\pi\alpha^2)/3s$ .

The  $\pi^-(\pi^+)$  structure function contains a valence part :

$$v^\pi(x_1) = \bar{u}_v^\pi(x_1) = d_v^\pi(x_1) = u_v^\pi(x_1) = \bar{d}_v^\pi(x_1)$$

and a sea part  $S^\pi(x_1)$  identical for  $\pi^+$  and  $\pi^-$  and assumed  $SU_3$  symmetric :

$$S^\pi(x) = \bar{u}_s^\pi(x) = u_s^\pi(x) = \bar{d}_s^\pi(x) = d_s^\pi(x) = s_s^\pi(x) = \bar{s}_s^\pi(x).$$

The nucleon has also a valence part  $u^P(x_2)(\equiv d^n(x_2))$ ,  $d^P(x_2)(\equiv u^n(x_2))$  and a sea part  $S^P(x_2)(\equiv S^n(x_2))$  taken  $SU_2$  symmetric with the assumption [9]

$$\bar{s}_s^P(x) = \frac{1}{2} \bar{u}_s^P(x) = \frac{1}{2} \bar{d}_s^P(x).$$

It is easily seen that by isospin invariance, the valence-sea, sea-valence and sea-sea terms are the same for  $\pi^+$  and  $\pi^-$  nucleon interactions. On the

other hand, the valence valence terms are different (roughly in the ratio  $(2/3)^2$  to  $(1/3)^2$  for  $\pi^-$  and  $\pi^+$  respectively). A global fit to  $\pi^+$  and  $\pi^-$  data thus allows a determination of both the valence and sea structure functions.

We use for the quark structure functions the following parametrization

$$V^\pi(x) = A^\pi x^{\alpha^\pi} (1-x)^{\beta^\pi}$$

$$S^\pi(x) = A_s^\pi (1-x)^{\gamma^\pi}$$

$$u^P(x) = A_u^P x^{\alpha_u^P} (1-x)^{\beta_u^P}$$

$$d^P(x) = A_d^P x^{\alpha_d^P} (1-x)^{\beta_d^P}$$

$$S^P(x) = A_s^P (1-x)^{\gamma^P}$$

We make the assumption  $\alpha_u^P = \alpha_d^P$  and  $\beta_d^P = \beta_u^P + 1$  which is the result of theoretical prejudices and supported by  $d(x)/u(x)$  measurement in DIS experiments which is well described by the parametrization  $d(x)/u(x) = 0.57 (1-x)$  [13]. The parameters  $A^\pi$ ,  $A_u^P$  and  $A_d^P$  are fixed in terms of  $\alpha$  and  $\beta$  by the normalization condition to the number of valence quarks :

$$\int_0^1 \frac{V^\pi(x)}{x} dx = 1 \quad \int_0^1 \frac{u^P(x)}{x} dx = 2 \quad \int_0^1 \frac{d^P(x)}{x} dx = 1$$

The average fractional momentum carried by gluons in the proton ( $\langle g^P \rangle$ ) and in the  $\pi$  ( $\langle g^\pi \rangle$ ) are deduced from momentum conservation :

$$1 - \langle g^P \rangle = \int_0^1 (u^P(x) + d^P(x) + 5S^P(x)) dx$$

$$1 - \langle g^\pi \rangle = \int_0^1 (2V^\pi(x) + 6S^\pi(x)) dx$$

The K factor is defined by the ratio [14] :

$$K = \frac{[d^2\sigma/dx_1 dx_2]_{\text{exp}}}{[d^2\sigma/dx_1 dx_2]_{\text{D.Y.}}}$$

In the following analysis, we will assume that  $K$  does not vary with  $x_1$  and  $x_2$ .

### 3.2 The Monte Carlo program

The simulation of the experiment is done using a Monte Carlo program. Dimuons are generated according to the Drell-Yan Model, starting from a given set of structure functions. The physical variables are :  $(x_1, x_2)$ , the transverse momentum  $P_T$ , the angular variables  $(\theta, \phi)$ . The transverse momentum is generated according to a parametrization of our data [7]; the acceptance being approximately independent of  $P_T$ , it does not critically depend on the specific form of the assumed  $P_T$  distribution. For the azimuthal angle, we assume a  $(1 + \cos^2\theta^*)$  distribution which is compatible with the one observed in our experiment [8]. The experimental set up is simulated including Fermi motion in the target nucleus, beam resolution, multiple scattering in the dump and measured inefficiencies of all detectors and trigger. The simulated events are processed through the same chain of analysis as data and the two dimensional  $(x_1, x_2)$  distribution of simulated events can be compared to the similar distribution of the data. The Drell-Yan cross section being rapidly decreasing with  $x_1$  (or  $x_2$ ), we have chosen a binning  $\Delta x_1(\Delta x_2)$  proportional to  $x_1(x_2)$  :  $\Delta x_1 = 0.05x_1$  and  $\Delta x_2 = 0.1x_2$ .

We use a likelihood estimator to compare the  $(x_1, x_2)$  distribution of data with the similar distribution of simulated events. As it is technically impossible to restart the full Monte Carlo simulation for each variation of the coefficients  $(\alpha^\pi, \beta^\pi, \gamma^\pi\dots)$  we have to determine, we introduce a parametrization of this simulation which also take into account the smearing effects of the measurement errors. We then search for the maximum of the likelihood estimator. We have checked by injecting the new set of parameters in a new Monte Carlo simulation that the method is rapidly convergent and gives the best estimate of the parameters of the structure functions after a couple of iterations.

### 3.3 Projection method

From the Drell-Yan formula, we can express the cross section for  $\pi$  as follows :

$$\frac{d^2\sigma}{dx_1 dx_2} = \frac{\sigma_0}{3x_1^2 x_2^2} [V^\pi(x_1) G(x_2) + S^\pi(x_1) H(x_2)]$$

where  $G(x_2)$  and  $H(x_2)$  take the following form, for platinum target ( $Z/A = 0.4$ ) :

$$G(x_2) = 1/9[1.6u^P(x_2) + 2.4d^P(x_2) + 5S^P(x_2)] \quad \text{for incident } \pi^-$$

$$G(x_2) = 1/9[0.6u^P(x_2) + 0.4d^P(x_2) + 5S^P(x_2)] \quad \text{for incident } \pi^+$$

$$H(x_2) = 1/9[2.2u^P(x_2) + 2.8d^P(x_2) + 11S^P(x_2)] \quad \text{for incident } \pi^\pm$$

To visualize the shape of the structure functions, we project the content of the  $(x_1, x_2)$  array on the two axes to get the distribution  $dN/dx_1$  and  $dN/dx_2$ . If  $L$  is the integrated luminosity calculated from the integrated beam intensity and from the useful number of nucleons assuming the measured linear  $A$  dependence [11] of the cross section, we can get an expression where only the variable  $x_1$  appears :

$$F_\pi(x_1) \equiv \frac{dN/dx_1}{\frac{\sigma_0 L}{3} \frac{1}{x_1^2} I^P(x_1)} = K \left[ V^\pi(x_1) + \frac{J^P(x_1)}{I^P(x_1)} S^\pi(x_1) \right] \quad (2)$$

in this equation  $I^P(x_1)$  and  $J^P(x_1)$  are integrals involving nucleon structure functions  $G(x_2)$  and  $H(x_2)$  and the calculated acceptance of the apparatus  $A(x_1, x_2)$  :

$$I^P(x_1) = \int_0^1 \frac{G(x_2)}{x_2^2} A(x_1, x_2) dx_2 \quad J^P(x_1) = \int_0^1 \frac{H(x_2)}{x_2^2} A(x_1, x_2) dx_2$$

The nucleon structure function can be expressed as a function of  $dN/dx_2$  in a similar form :

$$F_N(x_2) = \frac{dN/dx_2}{\frac{\sigma_0 L}{3} \frac{1}{x_2^2} I^\pi(x_2)} = K \left[ G(x_2) + H(x_2) \frac{J^\pi(x_2)}{I^\pi(x_2)} \right] \quad (3)$$

where

$$I^\pi(x_2) = \int_0^1 \frac{V^\pi(x_1)}{x_1} A(x_1, x_2) dx_1 \quad J^\pi(x_2) = \int_0^1 \frac{S^\pi(x_1)}{x_1} A(x_1, x_2) dx_1$$

This method does not allow to introduce any smearing due to uncertainties.

#### 4) RESULTS

##### 4.1 $\pi^+$ , $\pi^-$ , p data simultaneous fit

We first perform a simultaneous fit of the  $\pi^+$ ,  $\pi^-$  and proton data at 200 GeV/c and extract the structure functions of the pion and the proton. We assume the same value of the K factor for the two pion induced reactions. This global fit allows a determination of the structure function totally independent of previous DIS measurements. The results are shown in table 2 with the corresponding error matrix. As in  $\bar{p}N$  and  $pN$  data [5] the nucleon structure functions obtained are in good agreement with the results of neutrino D.I.S experiment [9], and this strongly enforces our assumption that the dimuon cross section does factorise as expected in the Drell-Yan model.

##### 4.2 $\pi^+$ , $\pi^-$ data fit

To improve the accuracy on the pion structure function, we fix the parameters of the nucleon structure functions at the values determined in D.I.S experiments including scaling violations [9]. A global fit to  $\pi^-$  and  $\pi^+$  data thus allows a determination of both the valence and sea structure functions. The obtained values of the parameters are given in table 3.

This fit provides the parameters of the pion sea structure function we shall use in the rest of the analysis.

We must combine the statistical errors quoted in table 3 with the systematical errors. The effect on the parameters of the different sources of systematical errors are the following :

- Nucleon sea structure function : CFS collaboration [12] determined a non SU2 symmetric nucleon sea structure function ( $\bar{u} \neq \bar{d}$ ). Using this result, we observe a variation on  $\gamma^\pi$  only.  $\Delta\gamma^\pi = -0.3$ .
- Error on relative luminosities  $\pi^-$  and  $\pi^+$  : a variation of  $\pm 2\%$  on the luminosities ratio give the following variation on the parameters :



$$\Delta\alpha^\pi = \pm 0.03 \quad \Delta\beta^\pi = \pm 0.02 \quad \Delta\gamma^\pi = \pm 0.7 \quad \Delta\langle g_\pi \rangle = \pm 0.04$$

Fig. 1a and b show the distribution  $F_\pi(x_1)$  (eq.2) and  $F_N(x_2)$  (eq.3) which visualise the pion and nucleon structure function respectively.

We obtain  $K = 2.3 \pm 0.5$ . The quoted error includes a relative error of 20% corresponding to the uncertainty of the  $\pi$  valence structure function (specially on  $\alpha^\pi$ ); uncertainty of 12% on the luminosity; and an error of 4% on the acceptance.

#### 4.3 150 GeV and 280 GeV data

A more detailed analysis of the valence structure function of the pion can be done using our high statistics data at 150 and 280 GeV/c. Since we have no  $\pi^+$  data at these energies, we cannot determine the pion sea and we use the value obtained at 200 GeV.

In order to compare the two samples of data at the same average mass squared :  $\langle M_{\mu\mu}^2 \rangle = 25 \text{ GeV}^2$ , we applied a mass cut  $4.2 \leq M_{\mu\mu} \leq 6.2 \text{ GeV}$  on the 150 GeV data and a mass cut  $4.2 \leq M_{\mu\mu} \leq 5.8 \text{ GeV}$  on the 280 GeV data. In this analysis, we also used  $Q^2$  dependant nucleon structure functions. The result of the fit is given in Table 4. The main sources of systematical errors are : the error on the pion sea structure function, the error on the proton sea structure function and the error on the acceptance of the apparatus. This last error is more important at 280 GeV/c than at 150 GeV/c.

Fig.(2a and b) and Fig.(3a and b) show the values of  $F_\pi(x_1)$  and  $F_N(x_2)$  at 150 GeV and 280 GeV respectively. We obtain also the two values of the K factor :

$$K(150 \text{ GeV}) = 2.49 \pm 0.37$$

$$K(280 \text{ GeV}) = 2.22 \pm 0.33$$

the indicated errors take into account the error on the pion valence structure function ( $\pm 7.5\%$ ), on the luminosity ( $\pm 12\%$ ) and on the acceptance ( $\pm 4\%$ ).

Combining these two measurements, we obtain the best estimate of the valence structure function of the pion at  $\langle M_{\mu\mu}^2 \rangle = 25 \text{ GeV}^2$  :

$$\alpha^\pi = 0.41 \pm 0.04 \quad \beta^\pi = 0.95 \pm 0.05$$

#### 4.4 Evolution of the structure function with $M_{\mu\mu}^2$

By a similar analysis with the two samples of data at  $\langle M_{\mu\mu}^2 \rangle = 50 \text{ GeV}^2$ , we can estimate the variation of the parameters  $\alpha^\pi$  and  $\beta^\pi$  between  $\langle M_{\mu\mu}^2 \rangle = 25$  and  $\langle M_{\mu\mu}^2 \rangle = 50 \text{ GeV}^2$  :

$$\Delta\alpha^\pi = \alpha^\pi(\langle M_{\mu\mu}^2 \rangle = 50) - \alpha^\pi(\langle M_{\mu\mu}^2 \rangle = 25) = 0.0 \pm 0.08$$

$$\Delta\beta^\pi = \beta^\pi(\langle M_{\mu\mu}^2 \rangle = 50) - \beta^\pi(\langle M_{\mu\mu}^2 \rangle = 25) = 0.15 \pm 0.08$$

Following the method proposed by Buras and Gaemers [10], we can determine the  $Q^2$  evolution of the non singlet structure function, parametrizing  $\alpha^\pi(Q^2)$  and  $\beta^\pi(Q^2)$  as :  $\alpha^\pi(Q^2) = \alpha^\pi(Q_0^2) + k_1 \bar{s}$  and  $\beta^\pi(Q^2) = \beta^\pi(Q_0^2) + k_2 \bar{s}$  with  $\bar{s} = \log((\log Q^2/\Lambda^2)/(\log Q_0^2/\Lambda^2))$ . For a given value of  $\Lambda$ , and from evolution equations, one can compute  $k_1$  and  $k_2$  and deduce the expected values of  $\Delta\alpha^\pi$  and  $\Delta\beta^\pi$  between  $M_{\mu\mu}^2 = 25$  and  $50 \text{ GeV}^2$  :

$$\text{for } \Lambda = 0.2 \text{ GeV} \quad \Delta\alpha^\pi = -0.01 \quad \Delta\beta^\pi = 0.07$$

$$\Lambda = 0.5 \text{ GeV} \quad \Delta\alpha^\pi = -0.01 \quad \Delta\beta^\pi = 0.10.$$

Despite the large error bars which make the result rather insensitive to the value of  $\Lambda$ , the experimental estimations of  $\Delta\alpha^\pi$  and  $\Delta\beta^\pi$  between  $M_{\mu\mu}^2 = 25$  and  $50 \text{ GeV}^2$ , indicate that our data are compatible with a scaling violation of the structure function.

## 5) CONCLUSION

We extracted the pion structure function assuming that the dimuon production cross section does factorize as predicted by the Drell-Yan model : the distinction between the valence and the sea of the pion is done at  $200 \text{ GeV}/c^2$  where we used incident  $\pi^-$  and  $\pi^+$ ; a precise determination of the valence of the pion is performed at  $150 \text{ GeV}/c^2$  and  $280 \text{ GeV}/c^2$  where we accumulated large statistics with incident  $\pi^-$ . The K factor measured at these energies lies in the range 2.2 - 2.5.

Finally, our data are compatible with scaling violation of the valence distribution inside the pion. The next generation of experiments with higher statistics should give a more precise measurement of this evolution over a wider mass range.

REFERENCES :

- [1] S.D. Drell and T.M. Yan; Phys. Rev. Lett. 25 (1970) 316;  
Ann. Phys. 66 (1971) 578.
- [2] H.D. Politzer, Phys. Rev. 70B (1977) 430; Nucl. Phys. B129 (1977) 301;  
C.T. Sachrajda, Phys. Lett. 73B (1977) 185;  
H. Georgi, Phys. Rev. D17 (1978) 3010;  
G. Altarelli, G. Parisi and R. Petronzio, Phys. Lett. 76B (1978) 351.
- [3] J. Kubar-André and F.E. Paige, Phys. Rev. D19 (1979) 221;  
G. Altarelli, R.K. Ellis and G. Martinelli, Nucl. Phys. B157 (1979) 461;  
J. Abad and B. Humpert, Phys. Lett. 80B (1979) 286;  
B. Humpert and W.L. van Neerven, Phys. Lett. 84B (1979) 327;  
85B (1979) 293; 89B (1979) 69;  
K. Harada, T. Kaneko and N. Sakai, Nucl. Phys. B155 (1979) 169;  
A.P. Contogouris and K. Kripfganz, Phys. Lett. B84 (1979) 473 and  
Phys. Rev. D19 (1979) 2207;  
J. Kubar et al., Nucl. Phys. B175 (1980) 251.
- [4] J. Collins, D. Soper and G. Sterman, Phys. Lett. 109B (1982) 388.  
G.T. Bodwin, S.J. Brodsky and G.P. Lepage, Preprint SLAC-PUB-2787;  
W. Lindsay, D.G. Ross and C.T. Sachrajda, paper submitted to 1982  
Paris Conference; and Southampton preprint.  
P.V. Landshoff and W.J. Stirling, Z. für Physik C14 (1982) 251.
- [5] J. Badier et al., Phys. Lett. 89B (1979) 145;  
J. Badier et al., Phys. Lett. 96B (1980) 422.
- [6] J. Badier et al., Nucl. Inst. and Methods 175 (1980) 319.
- [7] J. Badier et al., Phys. Lett. 117B (1982) 372
- [8] J. Badier et al., Z. für Physik C 11 (1981) 195.
- [9] J.G.H. de Groot et al., Phys. Lett. 82B (1979) 456;  
J.G.H. de Groot et al., Z. für Physik C1 (1979) 143.
- [10] A.J. Buras and K.J.F. Gaemers; Nucl. Phys. B132 (1978) 249.
- [11] J. Badier et al., Phys. Lett. 104B (1981) 335.
- [12] A.S. Ito et al., Phys. Rev. D23 (1981) 604.
- [13] F. Eisele, Structure functions, Proceedings of the XXI Int. Conf. on  
High Energy Physics, Paris (1982) 337.
- [14] The first determination of the K factor has been obtained in the  
following publications :  
J. Badier et al., Experimental determination of the pion and nucleon  
structure functions by measuring high mass muon pairs, Proc. EPS  
Intern. Conf. on High Energy Physics (Geneva 1979), CERN Preprint 79-67  
J. Badier et al., Phys. Lett. 89B (1979) 145.

TABLE 1

Number of dimuon events collected at 150, 200 and 280 GeV on the 6 cm Pt target in the mass interval 4.2 to 8.5 GeV/c<sup>2</sup>

P <sub>inc</sub>	Particle	No. Events	Luminosity (cm <sup>-2</sup> )
150 GeV/c	$\pi^-$	15 768	$5.0 \pm 0.7 \cdot 10^{38}$
200 GeV/c	$\pi^-$	4 961	$11.4 \pm 1.3 \cdot 10^{37}$
	$\pi^+$	1 767	$8.8 \pm 1.0 \cdot 10^{37}$
	p	1 048	$11.9 \pm 1.5 \cdot 10^{37}$
280 GeV/c	$\pi^-$	11 559	$2.8 \pm 0.3 \cdot 10^{38}$

TABLE 2

Result of a global fit of the  $\pi^+$ ,  $\pi^-$ , protons 200 GeV data.

		NA3 : 4.2 < M <sub><math>\mu\mu</math></sub> < 8.5 GeV						C.D.H.S. Q <sup>2</sup> = 20 GeV	
		$\sigma$	Correlation coefficients						
			$\alpha_u^p$	$\beta_u^p$	$\gamma^p$	$\langle g_p \rangle$	$\alpha^\pi$	$\beta^\pi$	$\gamma^\pi$
Proton	Valence	$\alpha_u^p = 0.57$	0.12						
		$\beta_u^p = 3.28$	0.27	.81					
	Sea	$\gamma^p = 9.33$	0.53	.29	.57				
		$\langle g_p \rangle = 0.43$	0.12	-.94	-.61	-.11			
Pion	Valence	$\alpha^\pi = 0.33$	0.14	-.80	-.62	-.18	.80		
		$\beta^\pi = 1.17$	0.10	-.44	-.35	-.08	.37	.35	
	Sea	$\gamma^\pi = 9.29$	2.6	.002	-.03	-.11	-.04	-.43	.27
		$\langle g_\pi \rangle = 0.55$	0.19	.70	.53	.20	-.66	-.33	-.16

TABLE 3

Improved fit of the pion structure functions  
at 200 GeV using  $\pi^+$  and  $\pi^-$  data.

		$\sigma$	Correlation coefficients		
			$\alpha^\pi$	$\beta^\pi$	$\gamma^\pi$
Valence	$\alpha^\pi = 0.45$	0.12			
	$\beta^\pi = 1.17$	0.09	.37		
Sea	$\gamma^\pi = 8.4$	2.5	-.22	.12	
	$\langle g_\pi \rangle = 0.47$	0.15	.02	.60	-.16

TABLE 4

Result of the fit of the pion valence structure function with the 150 GeV and 280 GeV  $\pi^-$  data at  $\langle M_{\mu\mu}^2 \rangle = 25 \text{ GeV}^2$ . The  $\pi$  sea and nucleon valence and sea structure functions are imposed.

		$\sigma$	Correlation coefficients	Systematical errors		
				pion sea	proton sea	acceptance
$\pi^- - 150 \text{ GeV/c}$	$\alpha^\pi = 0.41$	.05		$\mp .03$	$\mp .01$	-
$4.2 \leq M_{\mu\mu} \leq 6.2 \text{ GeV}$	$\beta^\pi = 0.92$	.04	.90	$\mp .01$	- .01	$\pm .02$
$\pi^- - 280 \text{ GeV}$	$\alpha^\pi = 0.41$	.05		$\pm .02$	+ .01	$\pm .01$
$4.2 \leq M_{\mu\mu} \leq 5.8 \text{ GeV}$	$\beta^\pi = 1.01$	.08	.87	$\mp .03$	- .02	$\pm .07$

FIGURE CAPTIONS

- Fig. 1a  $\pi^-$  200 GeV data. The data points represent  $F_{\pi}(x_1)$  as defined by eq. (2) using nucleon structure functions from CDHS fit.
- dashed curve represents the valence structure function of the pion obtained from our fit.
  - solid curve represent the (valence + sea) pion structure function as defined by eq. (2).
- Fig. 1b The data points represent  $F_{\pi}(x_2)$  as defined by eq. (3).
- dashed curve represent the valence part of the nucleon structure function  $1.6u(x_2) + 2.4d(x_2)$  for  $\pi^-$ .
  - solid curve represent the (valence + sea) nucleon structure function as defined by eq. (3).
- The curves have been scaled up by a factor  $K = 2.3$ .
- Fig. 2a  $\pi^-$  150 GeV data. The data points represent  $F_{\pi}(x_1)$  as defined by eq. (2) using nucleon structure functions from CDHS fit.
- dashed curve represents the valence structure function of the pion obtained from our fit.
  - solid curve represent the (valence + sea) pion structure function as defined by eq. (2).
- Fig. 2b The data points represent  $F_{\pi}(x_2)$  as defined by eq. (3).
- dashed curve represent the valence part of the nucleon structure function  $1.6u(x_2) + 2.4d(x_2)$  for  $\pi^-$ .
  - solid curve represent the (valence + sea) nucleon structure function as defined by eq. (3).
- The curves have been scaled up by a factor  $K = 2.49$ .
- Fig. 3a  $\pi$  280 GeV data. The data points represent  $F_{\pi}(x_1)$  as defined by eq. (2) using nucleon structure functions from CDHS fit.
- dashed curve represents the valence structure function of the pion obtained from our fit.

- solid curve represent the (valence + sea) pion structure function as defined by eq. (2).

Fig. 3b The data points represent  $F_{\pi}(x_2)$  as defined by eq. (3).  
- dashed curve represent the valence part of the nucleon structure function  $1.6u(x_2) + 2.4d(x_2)$  for  $\pi^-$ .  
- solid curve represent the (valence + sea) nucleon structure function as defined by eq. (3).  
The curves have been scaled up by a factor  $K = 2.22$ .



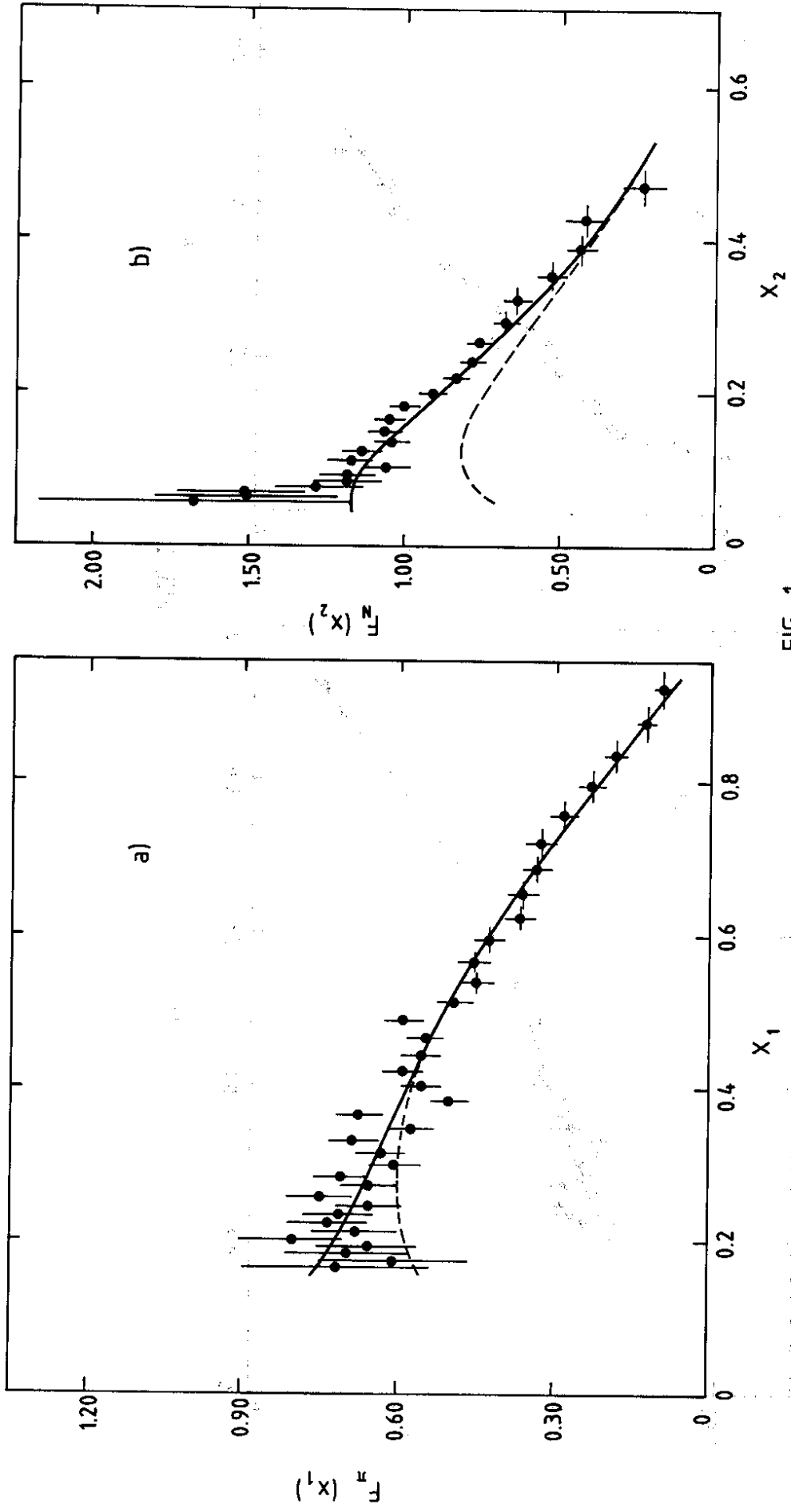


FIG. 1

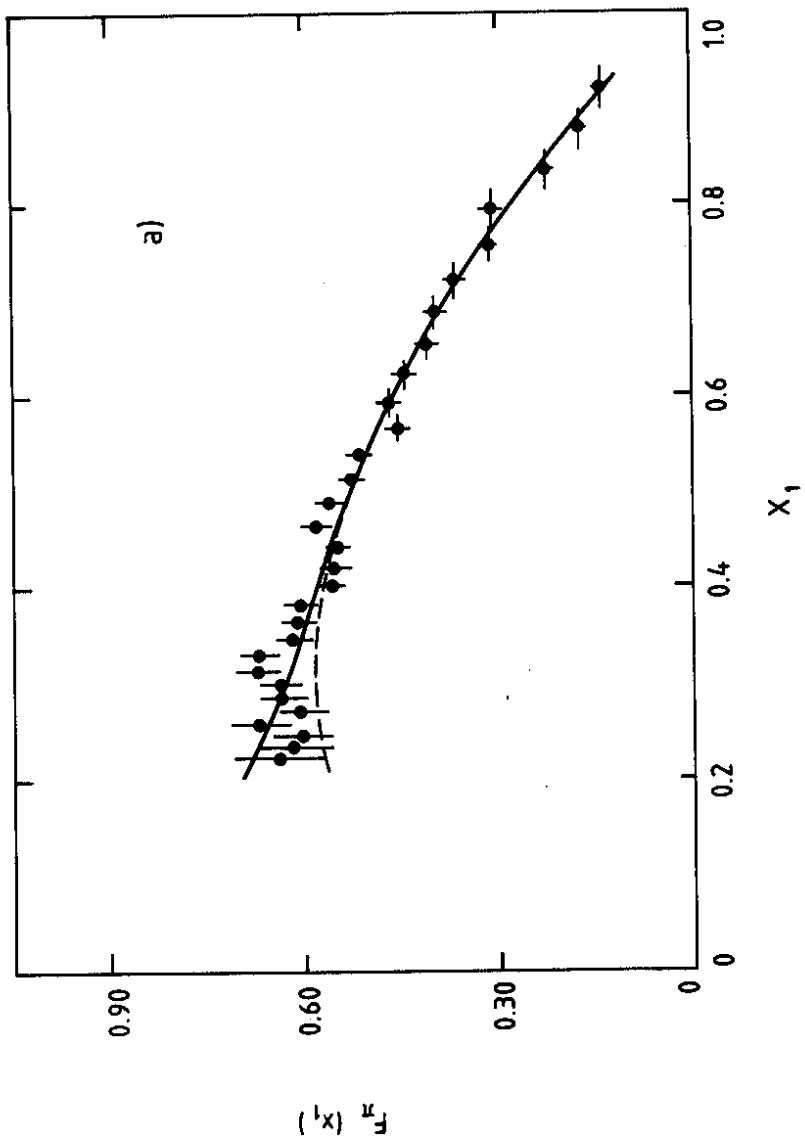
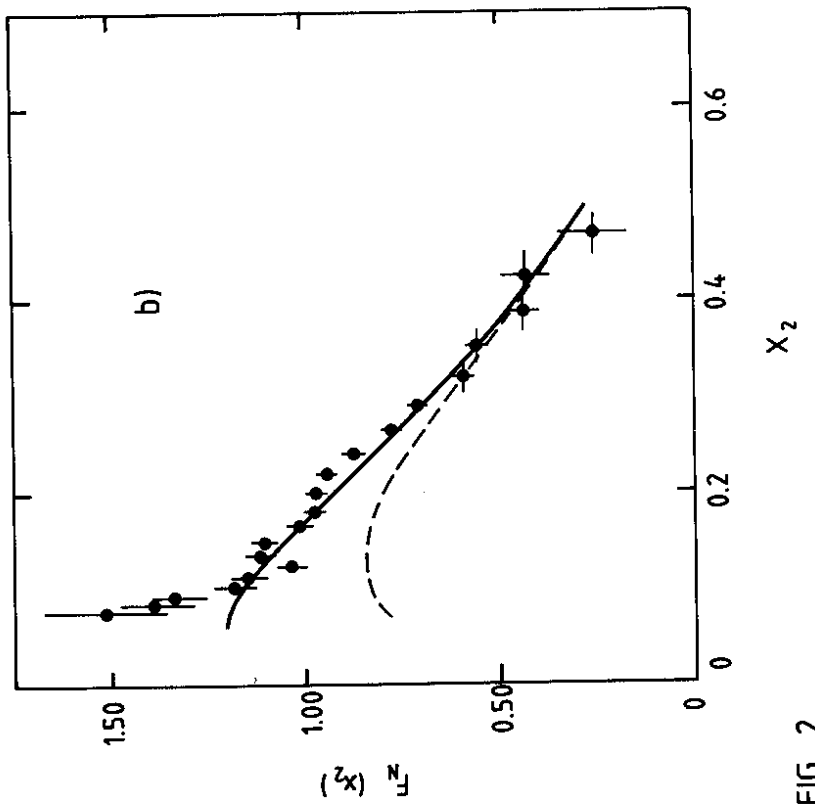


FIG. 2

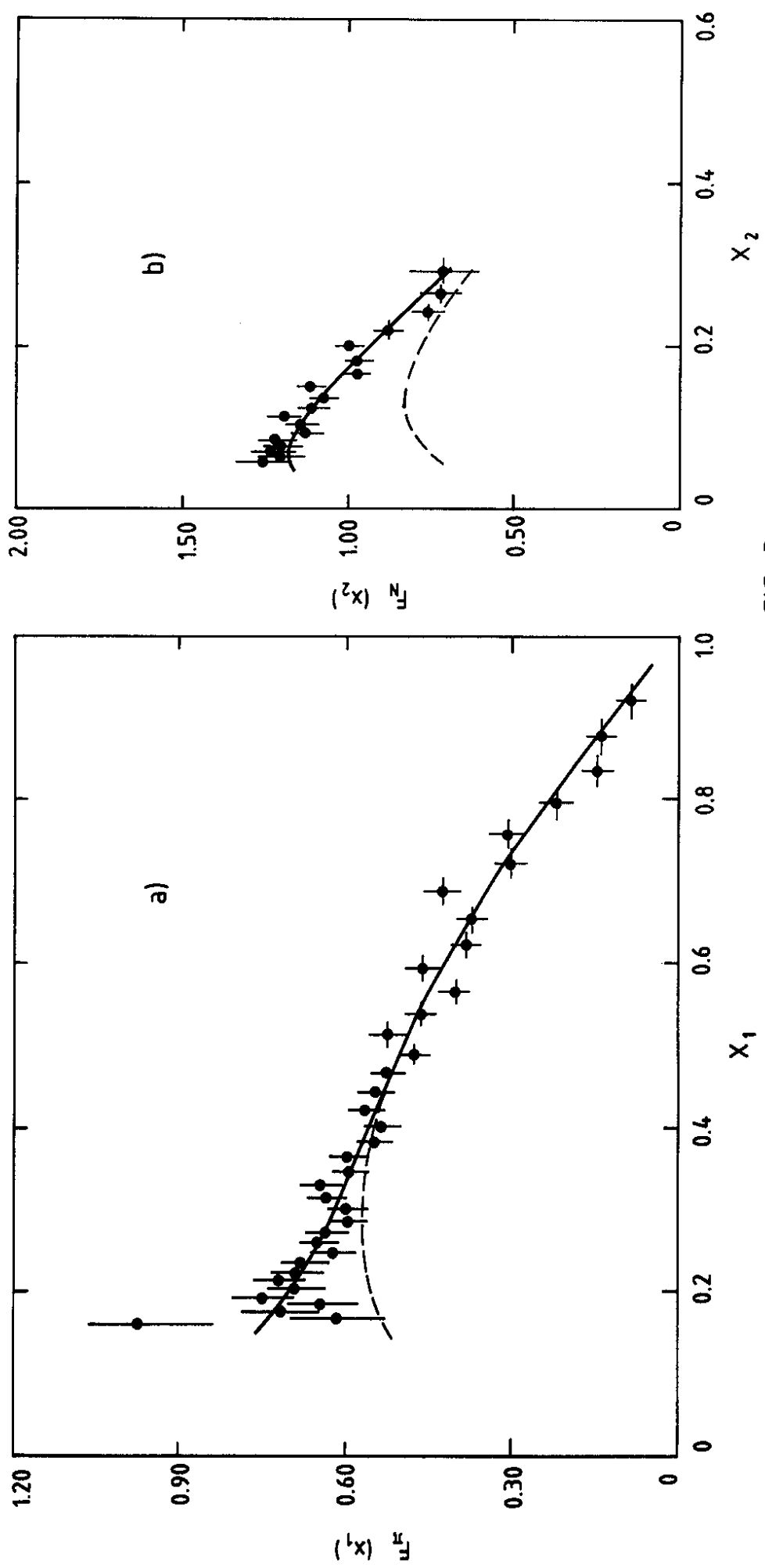


FIG. 3

